DR# 0116-3

Energy

FOSSIL

DOE/ET/11304-29
(DE84006656)

DEVELOPMENT OF MOLTEN CARBONATE FUEL CELL TECHNOLOGY

Technical Progress Report for the Period July—September 1983

Work Performed Under Contract No. AC02-76ET11304

Energy Research Corporation
Danbury, Connecticut

Technical Information Center
Office of Scientific and Technical Information
United States Department of Energy

DISCLAIMER

DISCLAIMER

This report has been reproduced directly from the best available copy.

Available from the National Technical Information Service, U. S. Department of Commerce, Springfield, Virginia 22161.

Price: Printed Copy A03
Microfiche A01

Codes are used for pricing all publications. The code is determined by the number of pages in the publication. Information pertaining to the pricing codes can be found in the current issues of the following publications, which are generally available in most libraries: *Energy Research Abstracts (ERA); Government Reports Announcements* and Index (*GRA* and I); *Scientific and Technical Abstract Reports (STAR);* and publication NTIS-PR-360 available from NTIS at the above address.

Printed in the United States of America
USDOE Technical Information Center, Oak Ridge, Tennessee

ENERGY RESEARCH CORPORATION

DOE/ET/11304-29
(DE84006656)
Distribution Category UC-93

DEVELOPMENT OF

MOLTEN CARBONATE FUEL CELL TECHNOLOGY

Technical Progress Report for the Quarter of July-September 1983

Prepared by

ENERGY RESEARCH CORPORATION

3 Great Pasture Road
Danbury, CT 06810

L. Paetsch, Program Manager

Prepared for the

UNITED STATES DEPARTMENT OF ENERGY

Chicago Operations and Regional Office
9800 South Cass Avenue
Argonne, IL 60439

Work performed under Contract No. DE-AC03-76ET11304

ACKNOWLEDGEMENT

The following individuals have contrtibuted to this report:

B. Baker
M. Benedict
R. Bernard
R. Chamberlin
J. Doyon
H. Maru
L. Paetsch
A. Pigeaud
A. Shah
M. Tarjanyi
P. Singh

EXECUTIVE SUMMARY

Component development during this quarter concentrated on two objectives: development of a creep resistance ribbed anode and development of an internal reforming catalyst for steam-methane reforming in the MCFC anode. Satisfactory anode creep strength has been achieved with Ni + 16 wt% LiAlO composite anodes. Efforts this period concentrated on fabrication methods to directly produce a ribbed anode from the Ni + $LiAlO_2$ powder mixture. Encouraging results were obtained by mold compression in a machined graphite mold followed by in-mold sintering which was promoted by the use of a few percent $LiKCO_3$ as a sintering agent.

Internal reforming catalyst development focused on preparation techniques for high surface area Ni catalyst supported on γ-$LiAlO_2$. The approach which is being most actively pursued involves first pelletizing the $LiAlO_2$ into suitable granule size followed by multiple impregnation in nickel salt solution and heat treatment. Several impregnations are necessary to obtain a nominal Ni loading of 15 weight percent. Out-of-cell catalyst testing has been initiated in planar integral reactors as well as differential tube reactors. The $LiAlO_2$ supported catalyst granules have demonstrated high activity for the methane-steam reforming reaction and kinetic parameters compare favorably with those for commercially available reforming catalysts.

Single cell testing is being conducted in support of anode development, thin matrix development and NiO cathode endurance testing. A 300 cm^2 size cell with a machined ribbed anode was tested for 1,000 hrs this period. Post-test analysis indicated excellent macro- and microstructural stability: 60 psi contact pressure on the ribs resulted in only 2 mil creep deformation (3.5%) and mean pore size increased by only 0.03 μm. A planar, creep resistant anode was operated in lab-scale cell no. 168 for 3,750 hours and again only 2 mil of creep deformation was measured.

Endurance testing of NiO cathodes is being performed to define the economic life of NiO and to identify practical means of extending life to satisfy economic endurance requirements. Post-test analyses of cells 161 and 168 indicate a correlation between electrolyte content in the cathode and NiO loss rate. Post-test analysis of a 7,000 hour bench-scale cell test, No. 7-40, gave evidence for a second sink for NiO deposition within the electrolyte tile. Besides reduction and precipitation of metal Ni particles near the tile center, bands of Ni and Fe oxides were also clearly

evident close to the tile-cathode interface. This observation suggests a NiO fluxing mechanism due to a negative solubility gradient for NiO within the catholyte.

Electrolyte matrix fabrication and testing activity has concentrated on tape cast matrix development. An economic process to produce controlled particle size γ-$LiAlO_2$ has been refined and progress has been made in selecting an optimum binary particle size mixture and ratio for high packing density (50-60% dense) and small mean pore size (<0.3 μm). Tape matrix shrinkage during binder burn-out can lead to stress cracking and several ways to minimize this shrinkage have been identified and verified in simulated cell tests. Solutions to the shrinkage problem include low tape porosity, thorough solvent removal prior to assembly and inclusion of partial electrolyte content in the tape. Pre-melting the partial electrolyte content onto the $LiAlO_2$ particles has been found to be a preferred electrolyte addition technique because of improved crack resistance during the electrolyte impregnation step.

TABLE OF CONTENTS

LIST OF FIGURES

LIST OF TABLES

TASK 1 COMPONENT DEVELOPMENT

Component development activities are concentrated on two objectives; development of a creep resistant, ribbed anode and development of an internal reforming catalyst structure for steam-methane reforming in the MCFC anode. High anode creep strength has been achieved with Ni + 16 wt% $LiAlO_2$ composite anodes. Efforts this period concentrated on fabrication methods to directly produce a ribbed anode from the Ni + $LiAlO_2$ powder mixture. Internal reforming catalyst development was involved in preparation techniques for $LiAlO_2$ supported Ni catalyst and out-of-cell screening of new catalyst structures. Catalyst pelletization and subsequent activation procedures have been established and out-of-cell testing in planar and tubular reactors indicates satisfactory activity for the methane reforming reaction.

1.1 Anode Development

Development of a creep resistant, ribbed anode structure continued during this reporting period. Two fabrication processes, tape casting and mold compression, are being developed in parallel as alternative approaches to production of physically mixed Ni + $LiAlO_2$ composite anodes. Ribbed anodes are being produced by machining thick sintered plaques and initial trials to direct fabrication of ribbed structures have been made with both the casting and molding techinques. Improved creep strength with reduced ceramic content in the anode is also being pursued through the use of smaller particle size ceramics and improved powder dispersion techniques.

Part of the tape cast anode fabrication process is the removal of the organic binders and plasticizers via low temperature burnout. It was found that after this burnout procedure the resultant anode plaque is strong and durable,

presumably due to the intimate Ni/$LiAlO_2$ particle packing inherent to this technique. Cell testing (Cell 170) of such a non-sintered anode was previously reported to have a 40 mV lower performance at 115 mA/cm^2 when compared to a similar cell test containing a 1000°C reduction sintered tape cast anode. Additionally, creep testing (standard conditions: 65 hrs., 700°C, 50 psi) of the sintered and non-sintered tape cast anodes showed the non-sintered structure to be weaker (12% creep) relative to the sintered structure (5% creep). Thus for the present time, sintering of tape cast anodes appears beneficial from the view points of cell performance and creep strength. If further testing indicates that a strong Ni/$LiAlO_2$ anode with acceptable cell performance can be manufactured without the reduction sintering step, then this will prove to be a simplified, cost-effective means of anode production.

Several thick planar Ni/$LiAlO_2$ plaques have been successfully fabricated using the tape cast and mold compression methods. Successful ribbed anodes have been fabricated by first tape casting a thick planar anode followed by machining to form the ribbed structure. One such ribbed anode (Figure 1.1) has been used in a bench-scale cell test which ran for 1000 hours with promising results (Cell 7-44). However, because of the need to make thick (~60 mils) planar structures for subsequent machining, problems have been encountered with the organic burnout step. The rate of burnout must be carefully controlled to avoid distortion and cracking. To avert this problem, direct tape casting into a ribbed substrate mold was attempted. However, a rippled and cracked structure resulted due to shrinkage during the drying of the non-uniformly thick body. Consequently, efforts to produce ribbed anodes will focus on the mold compression technique.

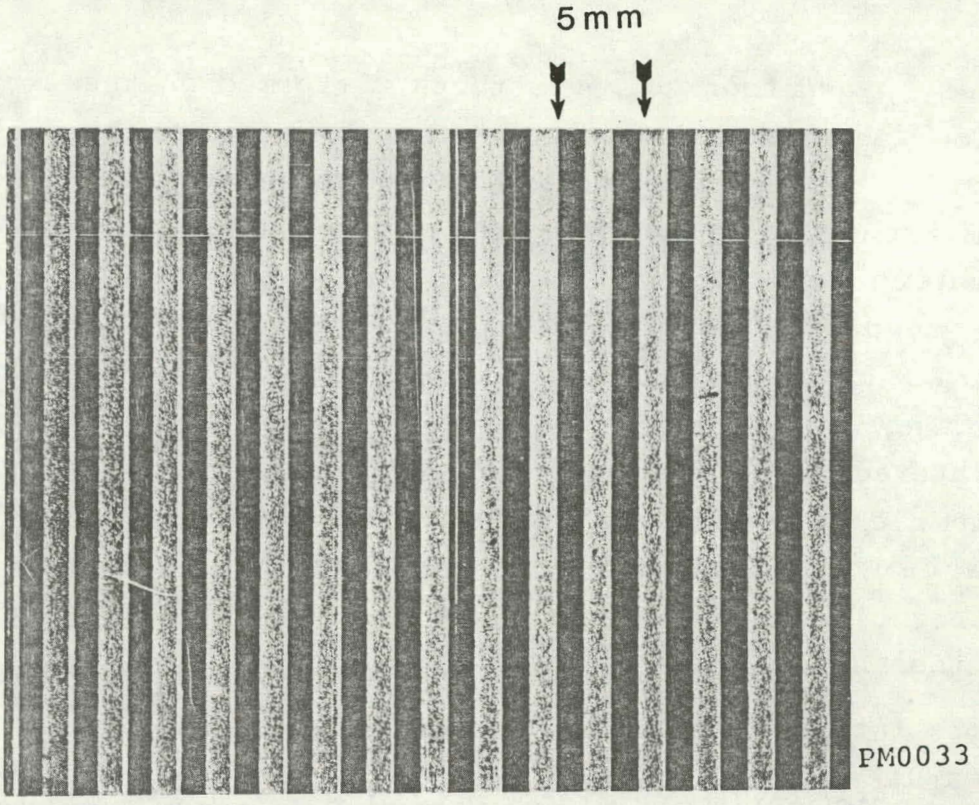

FIGURE 1.1 MACHINED RIBBED ELECTRODE

The efforts to direct mold a ribbed anode included trials to remove a green compact from the mold. Experiments using Ni/$LiAlO_2$ powder incorporating a binder were unsuccessful because the web and rib portions of the anode separated in each of several attempts. Additionally, an attempt at in-mold sintering using the binder additive powder did not work. However, attempts at in-mold sintering of a $LiKCO_3$ containing powder showed encouraging results. Although the linear shrinkage during sintering caused significant cracking in the structures "web", small pieces of intact ribbed electrode could be removed from the mold. Further trials using different extents of compaction, quantities of $LiKCO_3$ and sintering conditions are necessary to make this technique feasible for direct ribbed anode production.

In addition to the efforts performed on the two fabrication techniques discussed above, some preliminary experimentation has been conducted in other anode production areas. Much smaller quantities of ceramic would be necessary to achieve comparable strength if it were better dispersed and of much smaller particle size. If ceramic particles are small and well dispersed on the nickel powder prior to sintering, they will be incorporated into the "necks" of the sintered structure. In this way they will be strengthening the nickel matrix more effectively and not just filling the large pores and thereby preventing their collapse. We are currently investigating ways of dispersing very fine aluminum oxide in our present tape casting procedure.

1.2 Internal Reforming Catalyst Development

During this quarter, the catalyst preparation and out-of-cell screening tests in methane reforming processes were the major activities.

- Catalyst Preparation

High specific surface area, adequate porosity, stability under MCFC operating conditions, etc., are some of the structural requirements of an internal reforming (IR) catalyst. Reforming catalysts are commercially available in various shapes and catalytic activities. However, one of the major concerns in employing commercial catalysts for internal reforming is the stability of the support. Lithium-aluminate has been used for many years in MCFC as an electrolyte matrix material with very satisfactory results. Hence, the most stable γ-lithium aluminate allotrope appears to be an attractive candidate as an alternative catalyst support.

Last quarter, three different catalyst formulations were prepared. In these fabrictaion trials, wet-milling was employed to homogenize γ-$LiAlO_2$ powders and various nickel

salts. The wet mix was slurry cast and allowed to dry in air to yield an "agglomerated mass" for subsequent thermal processing and activation. As will be shown later, this preparation technique resulted in catalysts exhibiting reasonably high activities in methane reforming reactions. However, the physical structure of all three formulations was unsatisfactory due to their poor strength and low bulk densities (~0.3-0.5 g/cc).

To insure efficient mass transfer and maximum dispersion of the active catalyst component, catalyst support structures should possess the highest possible porosities consistent with strength and other requirements. Generally, commercial reforming catalyst structures attain this condition at ~50% porosities. Since the strength of an IR catalyst is only of secondary importance, the limit to increasing the porosities is dictated by physical and chemical stabilities.

During this quarter a new method of catalyst preparation was initiated which entails the preparation of porous lithium-aluminate structures prior to catalyzation. Samples of γ-$LiAlO_2$ powder were blended with a variety of binders. After drying, as required, the resultant blends were cold-pressed into discs or pellets (1.5 in. dia., 0.12 in. thick), and then sintered first in air at 650-700°C followed by further heat treatment in CO_2/air at 950-1000°C. Figure 1.2 typifies the porous sinters obtained with this preparation technique. Differences in the starting (green) densities are retained through the thermal treatment and a broad range of porosities can be obtained by proper selection of the initial pressing conditions. The sintered pellets and, for comparison, a tape cast layer were catalyzed by a chemical impregnation technique. Typical catalyst loading obtained with this technique is 15 weight% Ni achieved in three successive impregnation steps.

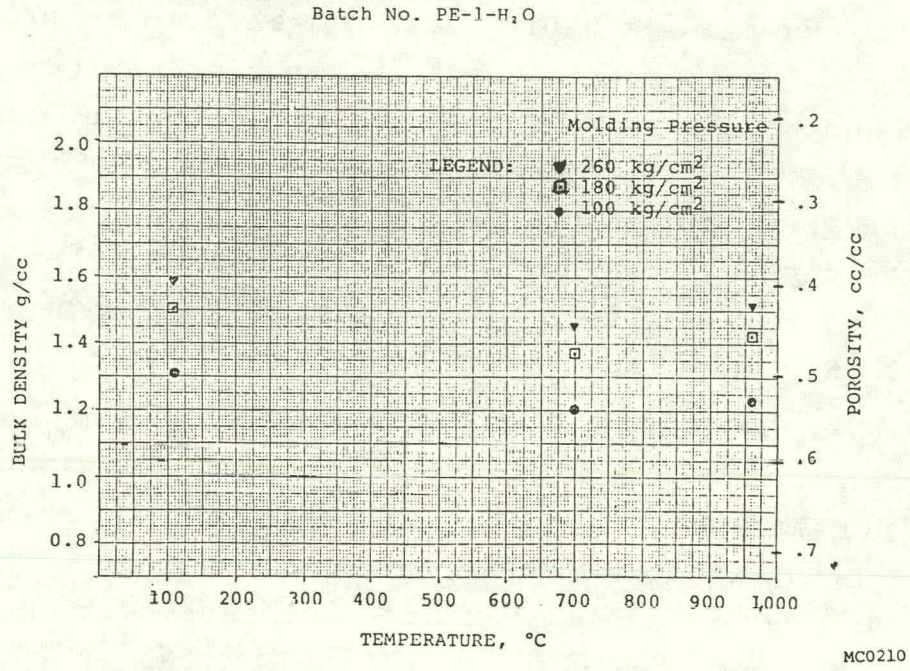

FIGURE 1.2 CATALYST SUPPORT PREPARATION

- Out-of-Cell Testing

Out-of-cell catalyst screening for methane conversion is carried out in two types of test systems:

1) In a planar reactor which simulates the conditions of MCFC with respect to gas flow distribution and catalyst bed loading, and

2) In tubular reactors operated under differential conditions which provide a more detailed kinetic information on catalyst activity.

This quarter, four out-of-cell tests were carried out in the planar reactor to evaluate the methane reforming activities of catalysts prepared by wet blending and by the impregnation technique discussed above. For testing, the catalyst granules were evenly spread into the cavities of a corrugated current collector prior to placing into the reactor. Typical catalyst loadings ranged from 13 to 24 mg/cm²

of projected area for wet blended catalysts and ~46 mg/cm² for the impregnated catalyst. Activation of the catalysts by reduction of the nickel oxide was carried out in all cases in the reactor in H_2 atmosphere at 650°C prior to reforming experiments.

Figure 1.3 illustrates the experimental results obtained for a wet blended catalyst at a steam to carbon ratio of 3.5, and at 250 and 490 HR^{-1} space velocities. Except for a temporary loss in activity monitored for the 270 hr and 280 hr tests (which was caused by carbon deposition) methane conversions close to thermodynamic equilibrium were achieved with this catalyst at both space velocities. Despite the notable initial reforming activities, the wet-milling technique for IR catalyst preparation seems to have limited merit at this time due to poor structural strengths and low densities.

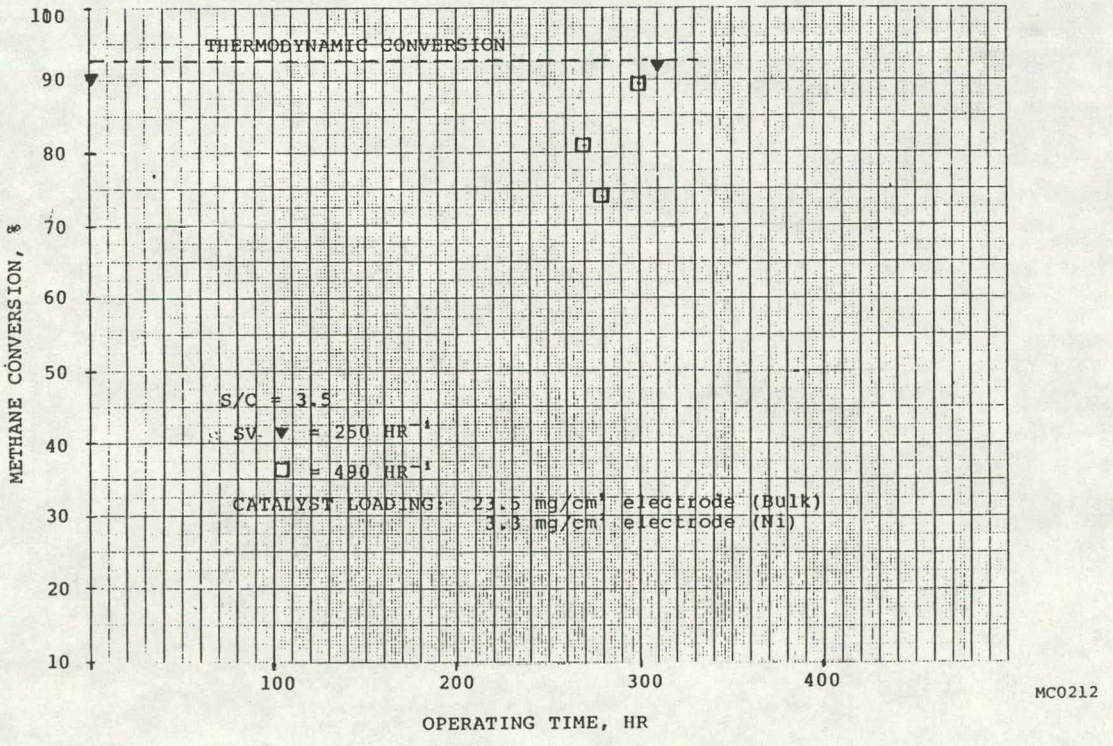

FIGURE 1.3 METHANE CONVERSION OUT-OF-CELL TEST (OCT-P-1)

Reforming activities measured at various steam to carbon ratios for a catalyst sample prepared during this quarter via the pelletization/impregnation technique are summarized in Figure 1.4. Examination of these data in conjunction with the operating time reveals that the reforming performance remained essentially stable up to 23 days and can be represented by the broken line as shown in this Figure. Compared

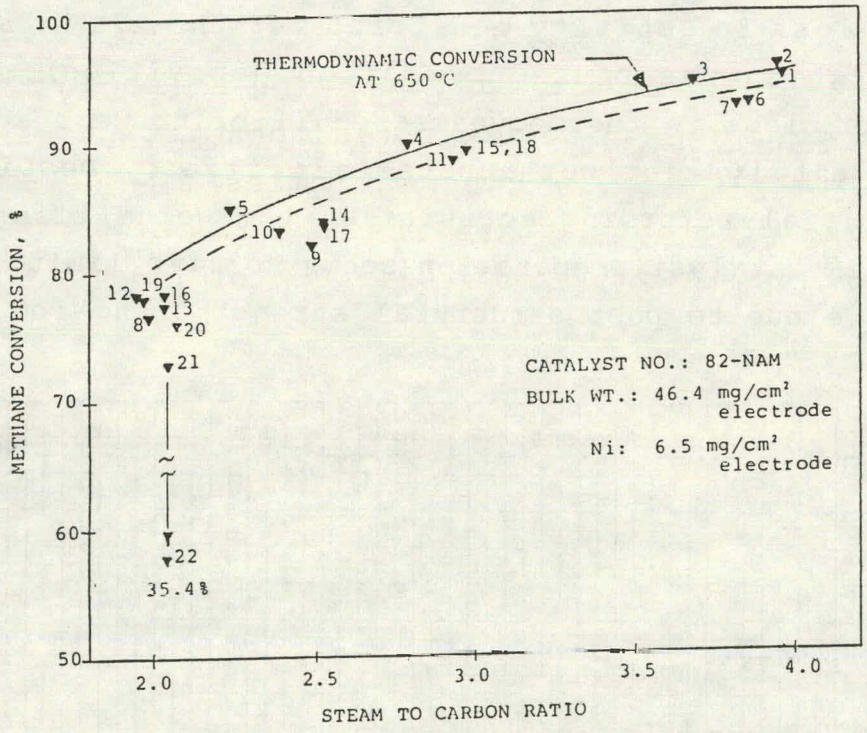

OPERATING TIME-DAY	DATA POINT-NO.
1	1
2	2
3	3,4,5
6	6,7
8	8,9
10	10,11,12
14	13,14,15
20	16,17,18
22	19
23	20,21
24	22

FIGURE 1.4 METHANE CONVERSION OUT-OF-CELL TEST (OCT-P4)

to the thermodynamic conversion (solid line), this represents less than 2% deviations from the theoretical values which could be accounted for by the experimental errors involved in measuring the various operating parameters. The performance decay commencing on day 23 was traced down to water supply and heating-control system malfunctioning. Hence, it is safe to assume that the present data is not representative of the maximum endurance levels obtainable with this catalyst structure.

Methane reforming tests employing a tubular reactor which is operated under differential conditions were also initiated this quarter. These studies are designed to characterize catalytic activities in terms of kinetic parameters with and without the presence of carbonate electrolytes and to determine the mechanism of catalyst deactivation.

Table 1.1 is a summary of the initial data obtained with a catalyst sample prepared during this quarter and which is also being tested in Cell 7-50. Reforming activities shown in this table for various temperatures indicate high catalytic activities which compare very favorably to commercial products. Experiments will continue and further reporting on results will follow.

TABLE 1.1 METHANE CONVERSION OUT-OF-CELL TEST (OCT-T-1)

Test Time	Temp. ^{o}C	A*	α** %	S/C	SPV Hr^{-1}
Start	650	550	56.9	2.36	5,030
1	600	363	43.0	2.33	5,190
	650	520	55.3	2.33	5,190
	700	750	68.6	2.33	5,190

*A: Catalyst activity $\frac{\mu\text{-mole } CH_4}{g\text{-sec-atm.}}$

**: Percent methane conversion.

TASK 2 SINGLE CELL TESTING

A 300 cm^2 cell with a machined ribbed anode was tested for 1000 hours this period. Post-test inspection revealed excellent structural stability of the anode; total shrinkage was 2 mil out of 57 mil with 60 psi rib compression. The effect of H_2 sintering on tape cast $Ni/LiAlO_2$ anodes was evaluated in lab-scale cells No. 168 and 170. Both cells displayed good performance stability, however, the H_2-sintered anode performed ~40 mV higher @ 115 mA/cm^2. Bench-scale cell 7-49 was assembled to evaluate the effect of cathode potential on NiO solubility. This cell will be operated at OCV and compared to a second cell operated at a current density of 160 mA/cm^2. Three bench-scale cells were assembled with tape cast matrices. One of these cells (7-46) contained a bubble barrier and showed no gas cross leakage for 1500 hours of operation. A summary of fuel cells tested during this quarter is presented in Table 2.1.

2.1 Endurance Testing of Anodes

- Bench-Scale Testing

Cell 7-44 was assembled to test a stabilized ribbed anode structure. This component was fabricated by tape casting a thick plaque of Ni + $LiAlO_2$ followed by burn-out in air, H_2 sintering at 1000°C and machining to form the ribbed structure. The as assembled anode was 57 mils thick with ribs that were 32 mils high by 63 mils wide. This cell was assembled with a standard SS reinforced cathode and hot pressed tile comprised of "in-situ" derived $LiAlO_2$ (mixed α, β, γ).

The cell was operated for 1000 endurance hours prior to voluntary termination for analysis of ribbed anode stability. The OCV of this cell was constant throughout the test (1.075V) with good wet seal efficiencies and no indication of cross-over. Cell ohmic resistance was normal and constant

TABLE 2.1 SUMMARY OF FUEL CELL TESTING

CELL NO.	LIFE (hrs)	PURPOSE	COMPONENT TYPE	POTENTIAL, mV @ 115 mA/cm² OCV V	PEAK (*)	AVERAGE	IR LOSS @ PEAK (mV)	COMMENTS
7-41	7000T	Eval. endurance of inconel-600 + thick NiO cathode	Matrix-H.P. tile Anode-Std. Ni/ $LiAlO_2$ Cathode-Dry Pack	1.076	853 (700)	810	66	Decay rate at 120 mA/cm² = 10 mV/1000 hrs
7-44	1000T	Eval. Tape cast anode w/ machined ribs	Matrix-H.P. Tile Anode-Tape Cast Ni/ 16 $LiAlO_2$ Cathode-Dry Pack	1.078	560	560	75	Low performance due to poor gas distribution - anode misalignment
7-45	4T	Eval. Electrolyte impregnation of tape cast matrix	Matrix-Tape Cast Anode-Std Ni/ $LiAlO_2$ Cathode-tape cast	-	-	-	-	Terminated due to cross leakage
7-46	1500T	Eval. tape cast matrix + bubble barrier	Matrix-tape cast Anode-Std Ni/ $LiAlO_2$ Bubble Barrier- tape cast Ni/ $LiAlO_2$ Cathode-dry pack	1.070	808 (640)	700	45	No x-over and No $CO_3^=$ additions For 1500 hours
7-47	250T	Eval. tape matrix fabricated with low cost $LiAlO_2$	Matrix-tape cast Anode-Std Ni/$LiAlO_2$ Cathode-dry pack	1.050	750	600	140	Cross Leakage
7-49	500	Eval. effect of cath. potential on NiO solubility	Matrix-H.P. Tile Anode-Std Ni/$LiALO_2$ Cathode-film cast	1.076	730	700	120	Operate @ OCV
168	3745T	Eval. creep resistance anode	Anode-tape cast Ni/$LiAlO_2$ Matrix-standard tile (mixed α,β,γ)	1.077	800	780	60	Good stable performance
170	2300T	Eval. non-sinter tape cast anode (simulate insitu binder burnout)	Anode-tape cast Ni/$LiAlO_2$ Matrix-standard tile (mixed α,β,γ)	1.070	760	745	68	Stable performance

(*) Potential at 160 mA/cm². 75% Fuel and 50% Oxidant Utilizations

beginning at 670 mΩ.cm² and ending at 605 mΩ.cm². As previously reported, cell performance was low due to maldistribution of fuel gas caused by an alignment problem which resulted in a gas bypass of the anode channels. Despite this problem, cell performance remained essentially constant throughout the 1000 hour test at 570 mV at 115 mA/cm².

Post-test inspection of the terminated cell revealed excellent dimensional stability of the anode. As shown (Figure 2.1) no deformation of the ribbed geometry occurred during 1000 hours with 60 psi contact pressure and total thickness decrease was only 2 mil out of the original 57 mil. Hg-intrusion porosimetry revealed little change in the pre and post-test pore spectrum with only 0.03 μm increase in MPS. Electrolyte fill level calculated from gravimetric

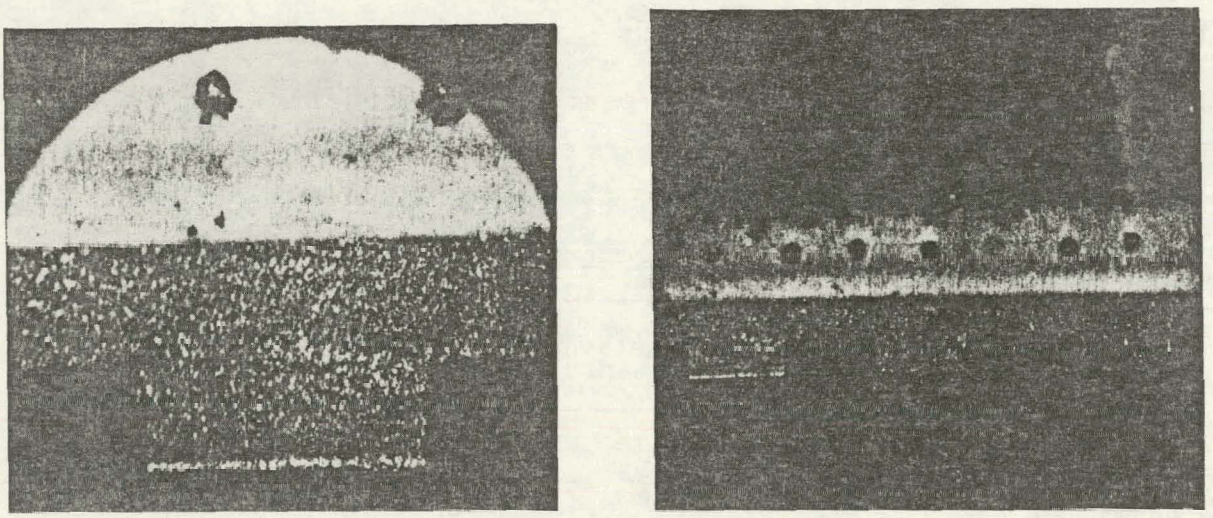

Thickness mil Pre/Post	Porosity % Pre/Post	Mean Pores μm Pre/Post	Electrolyte Fill, vol % of void Pre/Post
57/55	54/50	0.85/0.88	38/44

PM0016

FIGURE 2.1 RIB DEFINITION AFTER 1000 HRS 60 PSI (CELL 7-44)

analysis of the washed anode indicated that ~44% of the anode void volume was filled with electrolyte. Based on these results it is apparent that this component exhibits excellent stability of both the micro and macro structure as well as exhibiting good electrolyte retention capabilities.

- Lab-Scale Component Screening

Cells 168 and 170 were assembled to evaluate the performance and effect of H_2 sintering on the tape cast, creep strengthened Ni + $LiAlO_2$ anode plaque. The same fabrication procedure was used to cast a thick plaque which was subsequently machined into a ribbed structure and tested in Cell 7-44. Both of these cells were voluntarily terminated this period for the purpose of post-test analyses. Cell 168, which contained a tape cast anode that had been H_2-sintered at 1000°C, accumulated 3750 hours of endurance while Cell 170, assembled with the non-sintered anode, accumulated 2000 hours prior to test termination.

A lifegraph comparing the performance of these cells is shown in Figure 2.2. As seen in the figure, cell resistances were normal and comparable for these cells and performance stability was very good for lab-scale cells and also comparable. Peak performance of Cell 168 (sintered anode) at 115 mA/cm² was 810 mV, approximately 40 mV lower than state-of-the-art dry packed anodes, probably due to a non-optimized pore spectrum. The 115 mA/cm² performance of Cell 170 (non-sintered anode) was generally 40 mV lower than that of Cell 168. Post-test analyses of anode pore structure and electrolyte fill have not yet been completed for Cell 170 and thus an explanation of the lower performance of this cell is not presently available. The structural stability of the anode of Cell 168 was encouraging for a 3750 hour test: Total

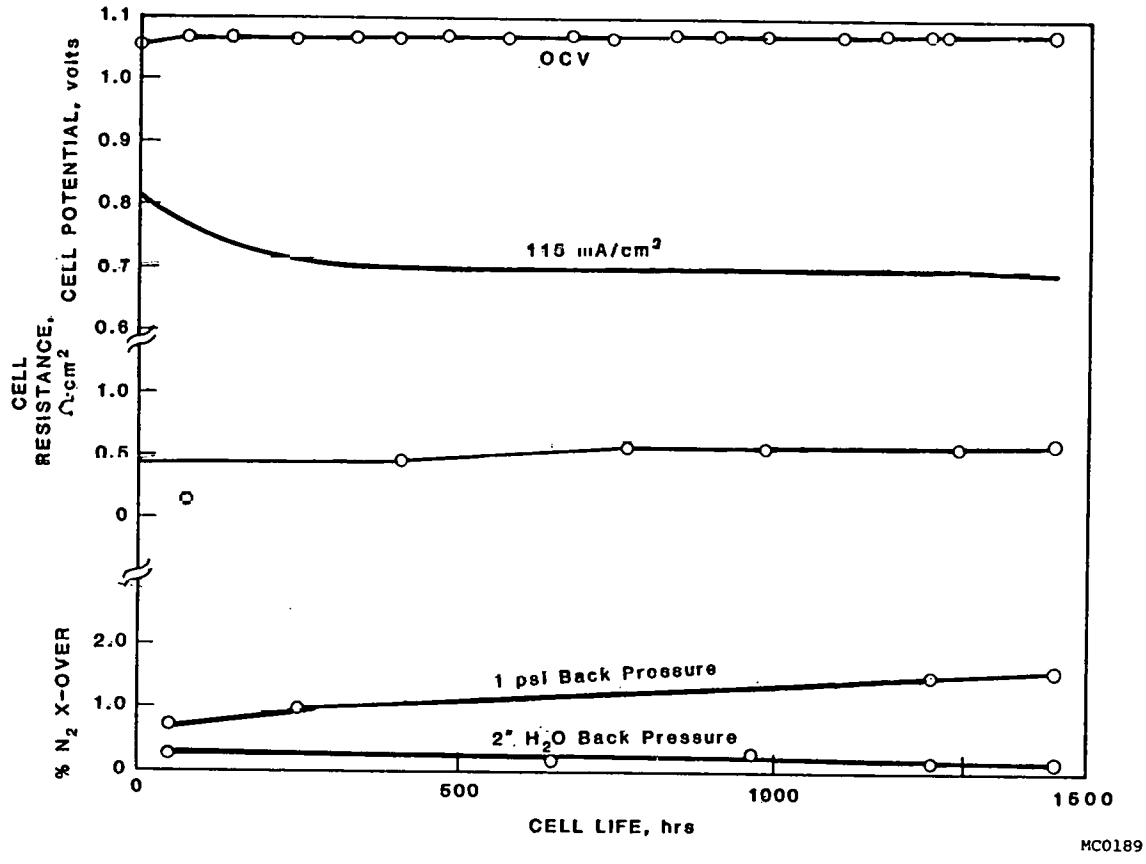

FIGURE 2.2 EFFECT OF SINTERING ON TAPE CAST ANODE PERFORMANCE

thickness decrease at contact points was 2 mil out of 22 mil, mean pore size increased from 0.9 to 1.0 μm, and post-test electrolyte fill was 61 vol% as opposed to a pre-test fill of 50 vol%.

2.2 Endurance Testing of NiO Cathodes

We are taking a three-fold approach to the endurance testing of NiO cathodes. One of these is out-of-cell testing, in which NiO solubility may be determined as a function of relevant parameters external to the cell environment. One object of such testing is the determination of conditions to minimize that solubility in order to apply them

to cell operation. A second phase involves the post-test analyses of cell components to evaluate the migration of NiO into the tile matrix as a function of time, comparison of this with theory, and the possible correlation with cell operating parameters. Finally, 7x7 in. bench-scale and 2x2 in. lab-scale cells are run to evaluate relevant changes in operating parameters and their effect on NiO solubility.

- Out-of-Cell Stability Tests

Three solubility test pots have been constructed during this period. They feature flat, flanged lid, sealed to the cell body with fibrous alumina gasket material. A cylindrical alumina crucible serves as a liner inside the pot. Into this is placed a conical alumina crucible containing the melt. Details of the sample container are shown schematically in Figure 2.3. Stirring of the melt and equilibrium

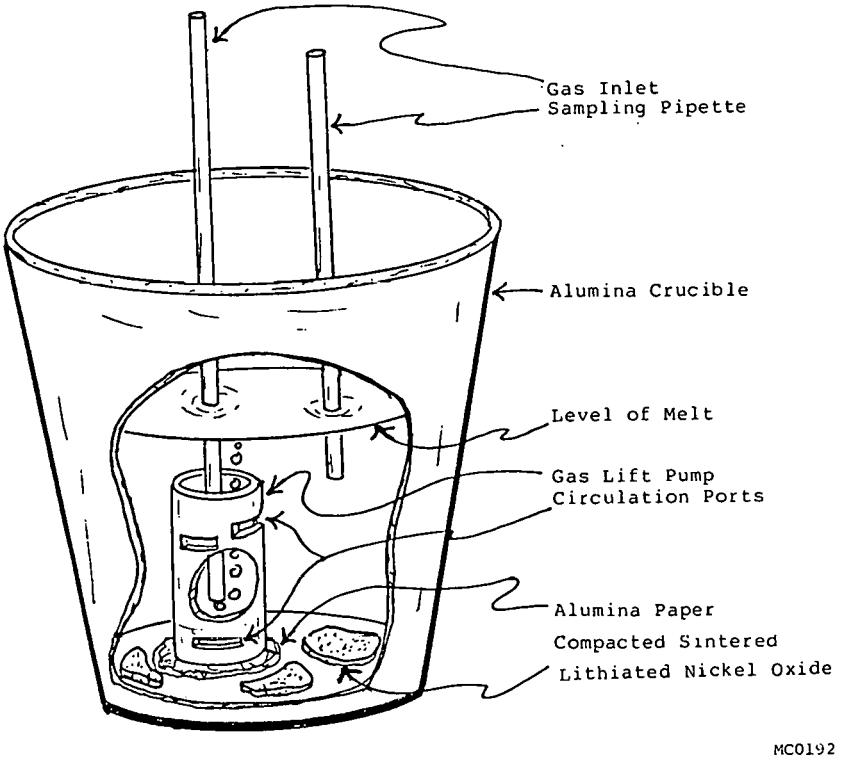

FIGURE 2.3 SOLUBILITY TEST APPARATUS

with the gas is done by bubbling the gas through an alumina tube into the gas lift pump assembly. This is a short length of alumina tubing which may project above the melt and has slots cut in it for circulation of the melt. It may be placed on a piece of alumina paper, or directly on the bottom of the crucible. The lithiated NiO will be in the form of compacted plaques. These can be protected further from crumbling and dispersal in the melt by a layer of alumina paper, if thought necessary. We feel that the stirring method given here will however ensure good thermal and chemical equilibrium, yet be gentle enough that no problems with particulate oxide will be encountered.

If, however, any problems are encountered with the inclusion of particulate materials in the sample, a modified sampling pipette may be used. A small filter tip made of Palau would be attached, perhaps with a gold or Palau wire, to the end of the alumina tube. The porous plug of Palau would need to have pores of the order of a few microns. The melt retained in this plug could not be retained as a sample, but only the amount in the alumina tube would be used.

The first "blank" run with the system is presently underway, using pure $LiKCO_3$ with a known amount of Ni added as a salt, for the purpose of testing it mechanically and perfecting the sampling techniques.

- Post-Test Analyses

Two cells, Nos. 161 and 168 were analyzed to determine the effect of electrolyte in the cathode on rate of dissolution if NiO. Cell 161 was prepared with components whose pore distribution would allow it to be run in "flooded" condition by frequent additions of electrolyte. Cell 168 was

constructed to be run "dry" with less frequent additions. Post-test analysis yielded the results in Table 2.2. A corrected analytical method has been used to revise the amounts of Ni determined.

It is obvious that the less the electrolyte present in the cathode the less the Ni in the tile at the end of the test.

The last column in the Table, the solubility, is estimated according to a model proposed recently[1].

For our purpose, we may take the model in the form

$$S = Ni \cdot f/D \cdot P_{CO_2} \cdot e^{1.5} \cdot t \cdot A$$

where
S = weight per unit volume of tile (geometric)
Ni = mass of Ni found
f = distance from cathode at which Ni is found
D = diffusivity of Ni ion
θ = porosity of the tile
t = time in seconds
A = frontal area

For the estimated solubilities in Table 2.2, f was assumed to be a planar front at 40 mils depth. θ was taken as 50%, and the exponentiated term is a tortuosity factor. P_{CO_2} was 0.33 atm, and D was taken [2] as 5×10^{-5} $cm^2 sec^{-1}$.

TABLE 2.2
EFFECT OF ELECTROLYTE FILL ON NiO DISSOLUTION

Cell	Life hrs	$CO_3^=$ Additions Grams	Cathode Fill, wt%	Ni in Tile $gmhr^{-1}cm^{-2} \times 10^6$	Estimated Solubility ppm
161	3100	2.3	15	7.9	63
168	3800	0.8	10	3.6	29

(1) United Technologies Corp., FCR-4515. Second Quarterly Report, Contract 5081-344-0528, Gas Research Institute, Aug 1982, p. 1-13.

(2) Delimarskii, Yu.K. and Tumanova, N.Kj., Ukr.Khim.Zh 29, 387-393 (1963); 30, 682-689 (1964); 30, 796-801 (1964).

It will be recognized that one could calculate a range of solubilities by assuming different values for the diffusion coefficient, the point at which the Ni precipitates in the tile, the porosity or tortuosity factor and the pressure of CO_2. A summary of such calculations is given in Table 2.3 for Cell 161, without, however, varying the CO_2 pressure. It is seen that a wide range of conditions could explain the data.

TABLE 2.3
CALCULATED SOLUBILITIES AS A FUNCTION OF MODEL PARAMETERS
Cell 161, @ 0.205 gm Ni, 3100 hrs

$D, cm^2 sec^{-1}$	Porosity, %	Precipitation Distance, mils	Solubility ppm
1×10^{-5}	30	10	168
		50	841
	50	10	78
		50	391
5×10^{-5}	30	10	34
		50	168
	50	10	16
		40	63*
		50	78
7×10^{-5}	30	10	24
		50	120
	50	10	11
		50	56

* Baseline, as shown in Table 2.2.

The model described here was apparently based on empirical correlations and no provision has been made for possible effects of P_{O_2}, P_{H_2O}, or activity of dissolved oxygen species. Considerations are presently underway to incorporate such features in a theoretical model. The important point here, however, is that the model was based on evidence,[1] somewhat supported by our data, that the diffusional transport of the Ni into the tile is the rate limiting step in the overall loss of nickel. It is therefore conceivable that some change of conditions in the chemistry which changes the solubility or diffusivity can make a beneficial change in the lifetime of the cell.

As an illustration, Table 2.4 shows the percentage losses expected with time from the cathodes tested, then shows the reduction we might expect by lowering the solubility by a factor of 2. The last column shows the life time of the cell assuming that a 20% weight loss is acceptable. It can be seen that in the best case, Cell 168 with the

TABLE 2.4
ESTIMATED LIFETIME OF CATHODES AS FUNCTION OF SOLUBILITY

Cathodes	Solubility ppm	Wt%, lost with time* 10,000 hr	50,000 hr	Hour for 20% Loss
161	63	15	73	14,000
	30	8	35	29,000
168	29	7	33	30,000
	15	3	17	59,000
LT-104	47	11	54	19,000
	25	6	27	37,000

* Avg. cathode weight, assumed, 4.5g.

limited amount of carbonate added, about 60,000 hours of life could be expected if the solubility could be halved. While these calculations are merely estimates, the results do imply that there may be hope for decreasing the Ni loss by adjusting the operation conditions of the cell.

- Bench-Scale Cells

Cell 7-40. This cell had operated for 7000 hours and some post-test analyses had been reported in the March quarterly report. In this past quarter, more extensive inspection of the Ni migration in the tile was done. Figure 2.4 shows schematically the cross-sectioned structure of the cell components observed by optical microscopy. Combined with Robinson backscatter SEM, EDAX, and X-ray dot maps, the following observations were made. First, there was extensive cracking in the transverse direction, and some delamination near the cathode. The cathode body was generally strongly adhered to the tile. Beginning beneath the sharp line of demarcation between the cathode and the tile, there was a

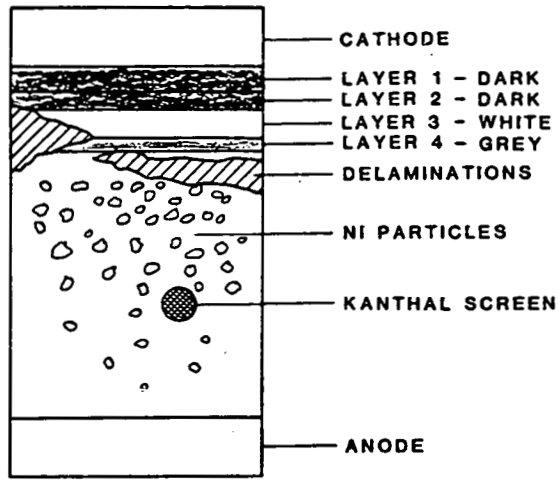

FIGURE 2.4 SCHEMATIC CROSS SECTION OF CELL 7-40

first layer of contamination which contained Fe, Ni, and K. A second such layer encapsulated a layer of white matrix material which, however, also contained Fe and Ni. Beneath this was a delaminated region of tile matrix containing Ni metal in relatively large agglomerated nodules. The remainder of the tile beneath this had Ni as smaller dots distributed throughout, but with the heaviest concentration in a band about 40-60% of the way through the tile. Between this band and the anode, the Ni dot map showed the Ni to be diffuse, but the tile contained relatively large amounts of Cr and Fe, presumably from the deteriorated Kanthal screen. It appears generally that the Ni is migrating through the tile, perhaps precipitating and redissolving, forming in distinct areas where chemical conditions are right. There was no continuous bridging of Ni found, and the deposits were globular rather than filamentary.

Some of the delaminated material at the interface between the cathode plaque and the main body of the tile was picked off and analyzed by XRD. The reflections obtained were compatible with gamma $LiAlO_2$ and NiO as major phases,

K_2CO_3 as minor phase, and traces of alpha Fe and $LiNiO_2$. There was some, not positive, indication of $CaCO_3$, Fe_2O_3 and $KAlF_4$. These results could mean that cathode material was strongly adhered to the interface although the samples seemed to be free of cathode plaque. They also could mean that the dissolved Ni reprecipitated as oxide in the first layer adjacent to the cathode. Analysis of the tile by AA found Ni in the amount of 2.3 gm $hr^{-1}cm^{-2}x10^6$. Traces of iron and chromium (0.008 and 0.26 gm $hr^{-1}cm^{-2}x10^6$ respectively) were also found. This is consistent with the results of the SEM and X-ray dot maps.

Cell 7-41: This cell was terminated this month after 7000 hours of operation. This cell, which was assembled with a thick (0.036") SS reinforced cathode, standard anode and hot pressed tile, exhibited state-of-the-art performance for the first several thousand hours. A summary of performance for this cell is presented in the lifegraph (Figure 2.5). Cell decay was uniform until at 7000 hours facility malfunction forced test termination.

Preliminary examination of the terminated cell revealed extremely clean and easily separable components. Severe hardware corrosion was absent although a large quantity of electrolyte was collected from the outside edge of the anode wet seal area. A detailed analysis of these components is planned, including a comparison of the cathode stability in these two (7-40, 41) recent 7000 hours tests.

Cell 7-49 was assembled during this period to evaluate the effect of cathode potential on NiO solubility. This cell, which was assembled with a film cast cathode, $LiAlO_2$ impregnated anode, and hot pressed tile, will be operated at OCV and compared to a second cell assembled with similar components which will be continuously operated at 75% fuel, 50% oxidant utilizations and 160 mA/cm^2 current density.

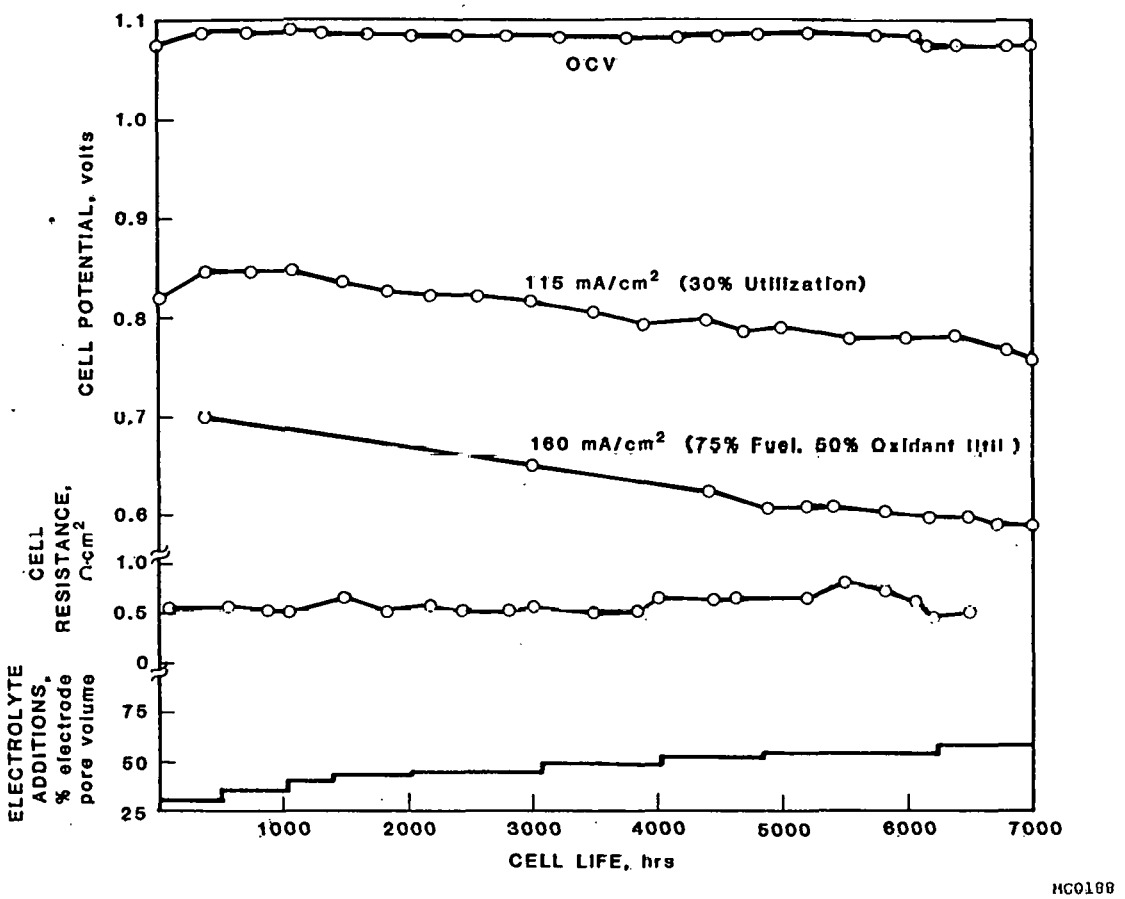

FIGURE 2.5 LIFEGRAPH CELL 7-41

Cell 7-49 exhibits a theoretical OCV for our gas composition and has near perfect gas seal efficiencies with no gas cross leakage through the matrix. Cell performance is ~150 mV lower than expected (850 mV) at 115 mA/cm² due to high resistance (60 mV) and large diffusion related anode polarization. The problem was traced to a faulty impregnation of the anode resulting in blockage of the gas side pores of the electrode with $LiAlO_2$ and electrolyte. Cell performance is improving due to electrolyte redistribution although state-of-the-art performance is no longer expected.

2.3 Electrolyte Matrix Fabrication and Testing

During the reporting period, progress has been made towards the production of desired surface area lithium aluminate (γ-$LiAlO_2$) powder at high yield rates for both internal reforming catalyst support activities and tape matrix fabrication. Tape cast matrix fabrication using various γ-$LiAlO_2$ particle sizes has also progressed along with the post matrix stability during binder burnout, structural integrity during electrolyte impregnation and electrolyte retention properties.

- γ-$LiAlO_2$ Production

Several batches of $LiAlO_2$ powders have been prepared under controlled experimental conditions and relatively high powder yield (more than 95% usable powder) has been obtained. Parameters such as Al_2O_3/Li_2CO_3 ratio, reaction temperature and exposure time have been found to influence the final powder surface area and particle growth and are being evaluated for the controlled production of both high (>10 m^2/g) and low (~1 m^2/g) surface area powders. Results to date indicate good reproducibility and ≃100% powder yield. Further results will be reported at a later date.

- Electrolyte Matrix Development

The goal of this task is to develop thin (20-25 mils thick) electrolyte matrix for carbonate fuel cell. The task consists of three major subtasks:

a) Development of a fabrication technique

b) Post fabrication characterization of the matrix

c) In cell tests of the matrix

Several batches of thin electrolyte matrix have been prepared successfully by tape casting technique during the reporting period. Matrices produced in general show uniformity in thickness, resistance to cracking during solvent evaporation and structural integrity during the removal of the substrate. Pin holes have been observed occasionally during the tape casting operation and is thought to be due to the presence of air bubbles in the casting slurry. Vacuum degassing of the milled slurry prior to casting has been found effective in reducing the occurrence of pin holes.

Post fabrication characterization of matrices includes the evaluation of matrix stability during binder burnout and electrolyte impregnation. Disc specimens selected randomly from tape matrices are heated up to 400-450°C in air to remove organics and then examined for cracks and deformation. To evaluate the behavior of matrices during electrolyte impregnation, disc specimens covered with electrolyte (to obtain 100% fill) are heated to 600-650°C and then examined for structural imperfections. A summary of matrix characterization is presented in Table 2.5. Pore spectrum (Figure 2.6) and mean pore size have also been obtained on matrices after binder burnout. The porosity and mean pore size of tape matrices prepared can be divided into two subgroups:

TABLE 2.5 MATRIX CHARACTERIZATION

TAPE NO.	POWDER BATCH SURFACE AREA m^2/g	d_{large} µm	d_{small} µm	MPS µm	TAPE POROSITY %	CARBONATE (VOL %)	CELL NO.	STRUCTURAL STABILITY
29	9.0		.25	.26	60.5	10	7-45	Expansion
30	9.0		.25	.19	58	0		Shrinkage
31	.34 + 6.4	6.7	.35	.23	55	0		Shrinkage
34	.34 + 3.4	6.7	.67	.38	50	0	7-46	Shrinkage
35	.15 + .34	15	.67	.64	50	0		Shrinkage
36	.15 + .34	15	.67	.94	50	25	7-47	Expansion
37	.34 + 3.4	6.7	.67	.55	43	25	7-48	Expansion
38	.34 + 9.1	6.7	.25	-	50	25		Expansion
39	.15 + 9.1	15	.25	1.5	48	25		Expansion
40	.15 + 9.1	15	.25	.6	45	25		Expansion
41	.15 + 3.48	15	.67	.65	47	15		Expansion
42	.15 + 3.48	15	.67	.55	47	10		Expansion

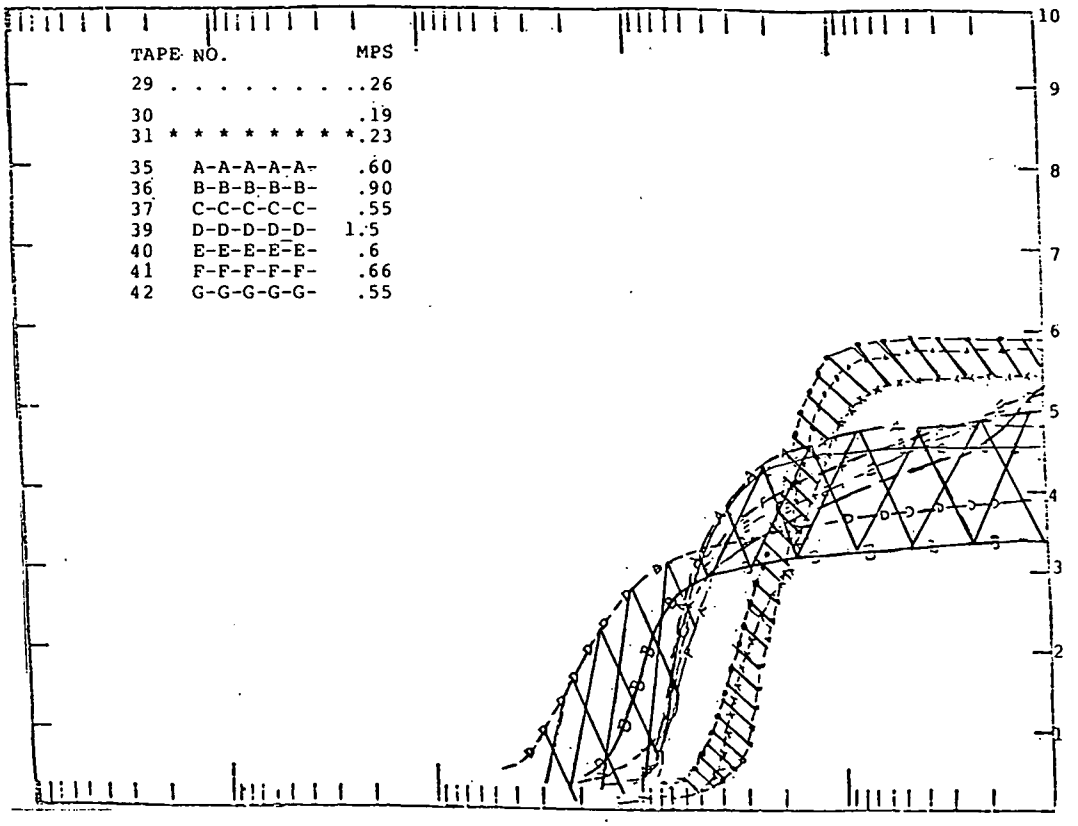

FIGURE 2.6 PORE SPECTRA OF MATRICES WITH DIFFERENT PARTICLE SIZE MIXTURES AND CARBONATE CONTENTS

a) Tapes with higher porosity and smaller mean pore size fabrication from higher surface area powders (singley hatched area).

b) Tapes with smaller porosity and relatively larger mean pore size fabricated from lower surface area and dual size powder mixtures (cross hatched area).

Lower porosity in matrices fabricated from dual particle mixtures is considered to be due to better packing of the interparticle voids (octagonal and tetrahedral voids). Larger mean pore size in these tapes is thought to be due to lower surface area of the powders. Work is in progress to characterize the effects of powder size on the mean pore size and porosity of the tape matrix and will be reported at a later date. It is also evident from the data that matrix shrinkage is eliminated by adding electrolyte to the slurry.

Several tape matrices have been tested in the cell. In general, thin matrices have been found to show poor electrolyte retention, leading to high crossover and poor cell performance. Poor electrolyte retention in the matrix is thought to be due to large pore size and improper pore distribution. Work is in progress to obtain smaller matrix mean pore size (~.25-.3 μm) along with higher tape density (55-60%) and will be reported at a later date.

- Matrix Testing

Three bench-scale (300 cm^2) cells have been assembled and tested during this period in support of tape matrix development. One of these, cell 7-46, was assembled with a tape matrix and a bubble barrier to evaluate endurance performance of these components. The other two bench-scale cells (7-45, -47) were assembled without bubble barriers in order to optimize the burnout and electrolyte impregnation cycle as well as evaluate the tape.

The testing of tape cast matrices has identified a problem with tape shrinkage during organic binder burnout. Since the tape matrix in a fuel cell assembly is restricted by hardware and component pinch,any shrinkage which occurs during binder burnout results in stress cracking and subsequent gas crossover. A series of in-cell and out-of-cell experiments identified several significant parameters which can minimize tape shrinkage. These parametes include:

- Low matrix porosity and hence a low organic content for low shrinkage.
- Pre-heating the tape at 150-175°C prior to assembly for complete solvent removal.
- Partial electrolyte content in the tape reduces shrinkage.

Two cells were assembled with a pre-dried tape matrix which was prepared with γ-$LiAlO_2$ and 7 wt% electrolyte with a solids density of 40% (60% porous matrix after organic burnout). The two cells were identical except for the quantity of electrolyte pre-stored in the anode. These cells were then slowly heated through the organic burnout cycle to a maximum temperature of 470°C (below the electrolyte melting point) and then cooled for examination of matrix shrinkage cracks. Both tapes were observed to be crack-free after the in situ burnout cycle and hence a reasonable confidence level was established for this tape matrix.

Cell 7-45 was assembled with the same tape matrix which was again pre-heated at 150°C. The intention of this cell test was to complete the in situ burnout and electrolyte impregnation cycle and continue heating to 650°C cell operating temperature to evaluate the tape matrix performance. After a four hour hold at 510°C impregnation temperature however, gas crossover was substantial and increasing. The cell was thus cooled down from 510°C for matrix inspection. On cell disassembly severe cracking of the matrix was observed. Cathode current collector corrosion was also noted. Gravimetric analyses of the post-test components before and after removal of the electrolyte were performed and the results are summarized in Table 2.6 below. It was concluded from these results that matrix cracking occurred

TABLE 2.6
ELECTROLYTE FILL LEVELS OF CELL 7-45

	Pre-test* Vol% of Void	Post-test Vol% of Void
Anode	50	36
Cathode	23	8
Matrix	100	83

* Pre-test electrolyte inventory is stored in anode gas chamber.

during electrolyte filling. This cracking could be caused by stress induced in the matrix as the electrolyte film coats closely packed $LiAlO_2$ particles.

It has also been suggested that because the electrolyte was added to the tape formulations as a powder, poor dispersion (of this powder) could result in the presence of large (>10 μm) agglomerates of carbonate which upon melting would leave corresponding pores in the $LiAlO_2$ matrix. For these reasons work was initiated on a tape matrix fabricated from $LiAlO_2$ particles that were precoated with an electrolyte film.

Cell 7-46 was the second bench-scale cell assembled for tape matrix evaluation. This cell contained a relatively dense matrix coupled with a bubble barrier on the anode side to eliminate initial crossover problems and thus enable performance and endurance evaluation of these components. This cell experienced no crossover problems and initial performance was satisfactory: 808 mV @ 115 mA/cm², 30% utilizations and 640 mV @ 160 mA/cm², 75% fuel and 50% oxidant utilizations (Figure 2.7). The effect of imposed pressure differential on gas crossover was analyzed by gas chromatography and results indicated proper functioning of the bubble barrier/matrix combination. A summary of performance is provided in Figure 2.8. As shown, the performance at 115 mA/cm² stabilized at ~700 mV after an initial decline during the first several hundred hours. Diagnostic analysis indicates that an unusually high diffusion related polarization was occuring at the anode. A review of the characteristics of this anode revealed a slightly lower than normal porosity and a higher than normal $LiAlO_2$ content, which could induce anode flooding. This cell exhibited no cross over problems.

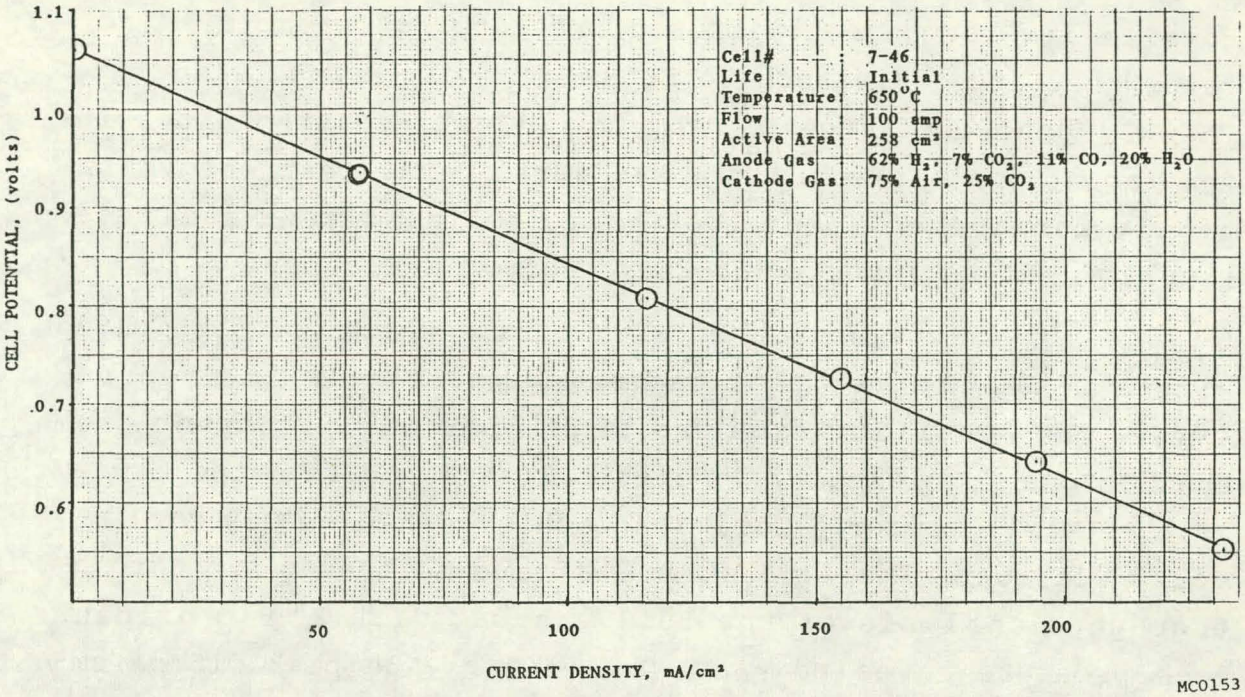

FIGURE 2.7 PERFORMANCE OF TAPE MATRIX WITH BUBBLE BARRIER (BENCH SCALE CELL 7-46)

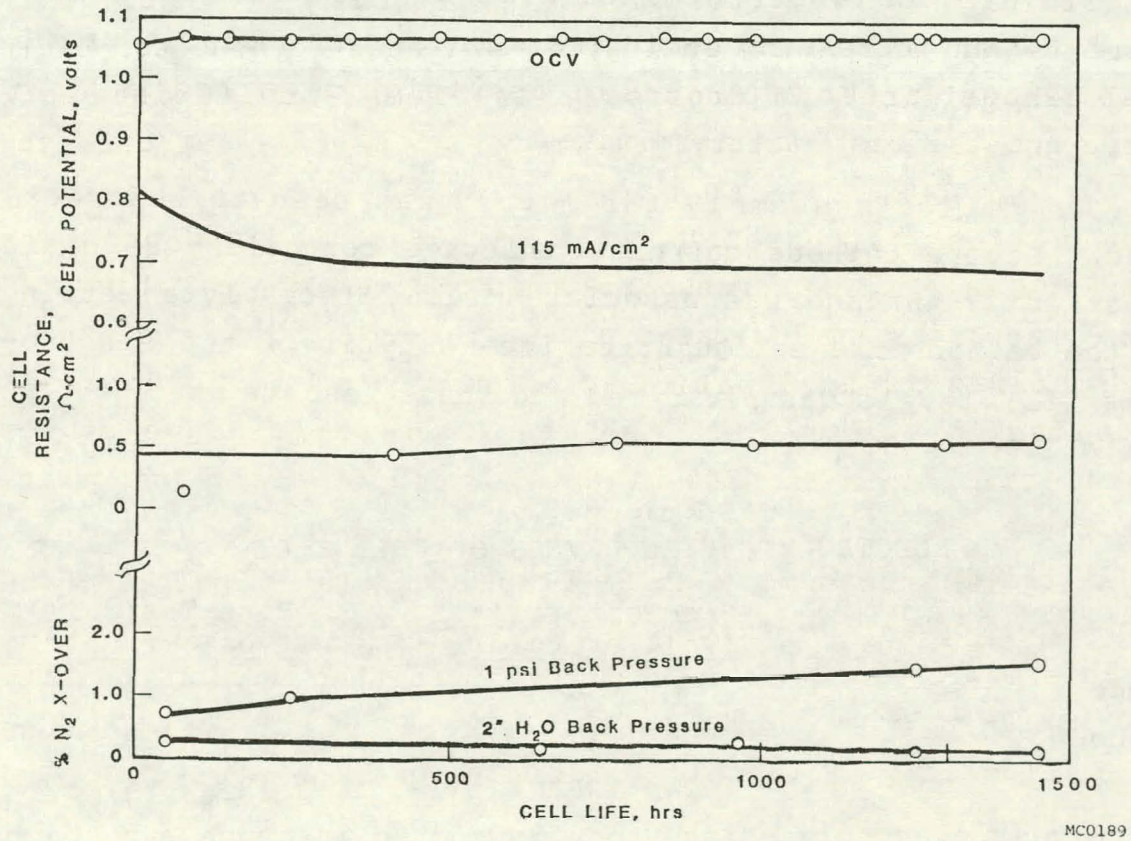

FIGURE 2.8 LIFEGRAPH OF CELL 7-46

However its response to imposed pressure differentials indicates that its resistance to cross over diminished with time. The OCV and resistance of this cell remained stable despite the fact that no electrolyte was added. The test was voluntarily terminated after 1500 hours for post-test analysis. Results will be reported as they become available.

Cell 7-47 was assembled with a tape which was fabricated with a $LiAlO_2$ powder that had been precoated with electrolyte. The resulting tape was significantly different from those tapes fabricated with electrolyte mixed into the slurry as a separate powder. Cell 7-47 achieved a peak OCV of 1.057 volts with our simulated steam reformed methane gas. Chromatographic analysis of the fuel exhaust with 2" H_2O oxidant back pressure revealed ~1.2% N_2 x-over. The peak 115 mA/cm^2 performance was 0.745 volts at 30% fuel and oxidant utilizations. After several days of operation the OCV began to deteriorate, cell performance also dropped and was accompanied by an increasing Ohmic resistance. An analysis of the fuel exhaust after 200 hours of operation revealed 5% N_2 x-over, and the test was terminated.

On cell disassembly the matrix was seen to be crack-free. Severe cathode current collector corrosion was again observed (7-45) and was associated with electrolyte wetting of the cathode frame. Quantitative analysis of the electrolyte fill levels was performed and these results are shown in Table 2.7

TABLE 2.7
ELECTROLYTE FILL LEVELS OF CELL 7-47

	Pre-Test Fill* (Vol% of Void)	Post-Test Fill (Vol% of Void)
Anode	50	59
Cathode	17	29
Matrix	100	74

* Pre-test electrolyte inventory is stored in anode gas chamber.

The post-test electrolyte fill levels shown above represent only a 3% loss of the total stored inventory. However, as the data shows, electrolyte drainage from the tile into the electrodes did occur. These results are consistent with the test data which showed a declining OCV and increasing Ohmic resistance. Analysis of this tape revealed that the $LiAlO_2$ powder had a lower than expected BET surface area while Hg-porosimetry indicated the after removal of the organics the tape had a larger than expected MPS. In conclusion, it is apparent that although tapes fabricated from this powder have good resistance to cracking, the matrix does not have a tight enough pore spectrum to retain electrolyte when coupled with our standard electrodes.